VIII CONGRESO IBÉRICO DE AGROINGENIERÍA 2015
RETOS DE LA NUEVA AGRICULTURA MEDITERRÁNEA
ORIHUELA-ALGORFA 1 a 3 de junio de 2015

Caracterización Avanzada de Tanques de Fermentación de Café mediante una Red Multidistribuida de Sensores RFID

Jiménez-Ariza, T.[1], Correa, E.C.[2,3], Díaz-Barcos, V.[3], Diezma, B.[2], Barreiro, P.[2], Arranz, F.J.[4]

[1] Universidad Agraria de Colombia - Uniagraria 1, 170, Bogotá, Colombia,

[2] Laboratorio de Propiedades Físicas y Técnicas Avanzadas en agroalimentación LPF-TAGRALIA. Universidad Politécnica de Madrid-CEI Moncloa, Av. Complutense s/n, Ciudad Universitaria, 28040 Madrid, Spain evacristina.correa@upm.es

[3] Dpto. de Química y Tecnología de los alimentos, Universidad Politécnica de Madrid-CEI Moncloa, Av. Complutense s/n, Ciudad Universitaria, 28040 Madrid, Spain

[4] Grupo de Sistemas Complejos, Universidad Politécnica de Madrid-CEI Moncloa, Av. Complutense s/n, Ciudad Universitaria, 28040 Madrid, Spain.

Resumen

La fermentación de las bayas de café se considera una etapa crítica en el procesado del café debido a su impacto en la calidad final del producto. La temperatura es una de las principales variables de control que puede ser utilizada para predecir el final del proceso, teniendo en cuenta que varios autores indican que el control de esta etapa es fundamental para evitar la mala calidad de la bebida final. En la práctica, la fermentación es el paso menos controlado del proceso, haciendo que los beneficiaderos operen lejos de sus condiciones óptimas en términos de costes de operación (es decir, elevados consumos de energía y agua) y de calidad del producto final.

El objetivo de este trabajo es caracterizar los gradientes de temperatura que se dan en los tanques de fermentación mediante una red multi-distribuida de sensores autónomos, inalámbricos y de bajo coste (registradores de temperatura del tipo RFID, identificadores de radiofrecuencia semipasivos modelo TurboTag®).Para ello se utilizan dos metodologías: la interpolación espacial en coordenadas polares y los diagramas de espacio de fase.

Se supervisaron dos fermentaciones reales de café, en El Cauca (Colombia), mediante sensores sumergidos directamente en la masa en fermentación. Los fermentadores eran tanques de plástico cubiertos, uno de ellos colocado en el interior de un almacén, permaneciendo el otro a la intemperie. El rango de variación máximo de temperatura en los tanques fue de 4,5ºC. La interpolación espacial mostró, incluso en el fermentador bajo las condiciones menos desfavorables en el interior del almacén, un gradiente radial de temperatura instantáneo de 0,1 °C/cm desde el centro hasta el perímetro del tanque y un gradiente vertical de temperatura de 0,25 °C/cm para sensores con coordenadas polares iguales. La combinación de ambas metodologías permitió la identificación consistente de los puntos calientes y fríos de ambas fermentaciones.

Palabras clave: Gradientes de Temperatura, WSN, Espacio de Fases, Interpolación Espacial, calidad

Advanced Characterization of Coffee Fermenting Tanks by Multi-distributed RFID Sensors

Abstract

The fermentation stage is considered to be one of the critical steps in coffee processing due to its impact on the final quality of the product. Temperature is one of the main control variables, which can be used to predict the end of the fermentation process. Several authors indicate that fermentation must be controlled to limit poor beverage quality. However, in reality, fermentation is the least controlled step of the process, causing production plants to operate far from optimal conditions in terms of both operation costs (i.e. high energy and water consumptions) and final product quality.

The objective of this work is to characterize the temperature gradients in a fermentation tank by multi-distributed, low-cost and autonomous wireless sensors (semi-passive TurboTag® radio-frequency identifier (RFID) temperature loggers). Spatial interpolation in polar coordinates and an innovative methodology based on phase space diagrams are used. Two real coffee fermentation processes were supervised in the Cauca region (Colombia) with sensors submerged directly in the fermenting mass. The natural fermentations of coffee were carried out in a covered plastic tank, one of them placed inside a warehouse and the other one remained in the open. Fermentations leading to a 4.5 °C temperature range within the fermentation process. Spatial interpolation shows a maximum instant radial temperature gradient of 0.1 °C/cm from the centre to the perimeter of the tank and a vertical temperature gradient of 0.25 °C/cm for sensors with equal polar coordinates, in the tank placed inside the warehouse. The combination of spatial interpolation and phase space graphs consistently enables the identification of different local behaviours during fermentations (hot and cold spots).

Keywords: Temperature gradients, WSN, Phase Space, Spatial Interpolation, Food Quality

Introduction

Coffee is one of the most popular and consumed food product in the world. According to the International Coffee Organization, during the 2012-2013 harvest, 145 million bags of 60 kg were produced globally. The quality of coffee beverage is strictly related to the chemical composition of the roasted beans, but also, to postharvest processing (Illy and Viani, 2005). To produce coffee beans suitable for transport and roasting there is a need of segregating the seeds from the outer layers. World-wide, coffee cherries are processed either by “dry” or “wet” method in order to separated the beans from the pulp. In Colombia, Central America and Hawaii, the wet method is preferred for Arabica coffee (Mussatto et al., 2011). In such case, coffee cherries are first depulped in order to remove the skin (exocarp) and the pulp (outer mesocarp), and then after a relative short period of fermentation (24-48 h) a water wash is used to remove the mucilage layer. The beans are then sun-dried to reach 12% moisture content. The main goal of fermentation is to degrade the slimy mucilage adhering firmly to coffee beans (Illy and Viani, 2005), mainly constituted of simple sugar and pectic substrate (Garcia et al., 1991), which are converted to alcohols and organic acids exothermically. The production of these metabolites leads to make a pH decrease (Avallone et al., 2001); a textural change is observed and washing can finally eliminate this mucilage. Masoud and Jespesen (2006) and Peñuela-Martinez et al. (2010) suggest as main control variables temperature and pH, which can be used to predict the end of the fermentation process. Several authors indicate that fermentation must be controlled to limit beverage miss quality (Bede-Wegner et al., 1997; Lopez et al., 1989; Murthy and Naidu, 2011; Woelore, 1993). But actually, fermentation is the least controlled step of the process, which leads production plants to operate far from optimal conditions both in terms of operation costs (i.e. high energy and water consumptions) and final product quality (Barreiro et al., 2010). Research efforts are being exerted, among others, in the development of novel, fast, non-destructive and accurate sensing techniques suitable for on-line process optimization and which could provide information highly correlated to quality properties (Esteban-Diez et al., 2004).

Only a few research, as those carried out by Avallone et al., (2001), Jackels et al (2005), Peñuela-Martinez et al (2010) and (Correa et al., 2014), are related to the control and supervision of coffee fermentation. References affecting automatic systems for controlling fermentations based on wireless sensors are mostly focused on wine. Among them Ranasinghe et al. (Ranasinghe et al., 2013) propose to measure temperature gradient across a fermentation tank with a sensor array constructed to accommodate seven wireless resistance temperature detectors capable of real-time monitoring of fermentation vats, while Di Gennaro et al and Sainz et al (Di Gennaro et al., 2013; Sainz et al., 2013) focus on wireless sensor communication issues.

The objective of this work is to characterize the temperature gradients in two fermentation tanks by multi-distributed, low-cost and autonomous wireless sensors by spatial interpolation in polar coordinates and an innovative methodology based on phase space diagrams.

Materials and Methods

Experimental setup

Coffee cherries (*Coffea arabica* var. Castillo, Borbón and Caturra) were hand-picked at the mature stage in a plantation from Popayán (Cauca, Colombia). External mesocarp was mechanically eliminated immediately after harvesting and depulped bean was left to natural fermentation. The fermentation begun when outside temperature decreases and the process ended according to expert inspection (Table 1).

Two natural fermentations of coffee were carried out in a covered plastic tank (Figure 1), having the shape of a frustum of a cone, placed outside under external ambient conditions (F_{OUT}) during the first fermentation and inside a warehouse (F_{IN}) during the second one. The tank with a top diameter of 1.04 m and height of 0.85 m was filled with depulped coffee cherries to a tank fill level of around 0.44 m (Figure 1). This set-up is one of the possibilities that can be found in the region of Cauca, where heterogeneous tank designs are used depending on the characteristics of each coffee farm.

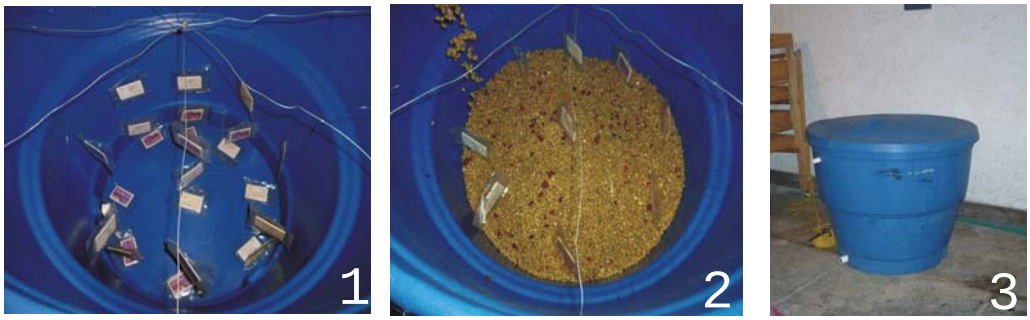

Figure 1. *Images of experiment setup: 1. placement of sensors, 2. filling the tank, 3. fermentation.*

Table 1. *Characteristics of the fermentations. Schemes of the sensors distribution in the tanks.*

Date Amount	Fermenter location	Sensors location	Sensors number	Temporal resolution	Fermentation time
May 2011 230 kg of depulped coffee cherries	 Outside	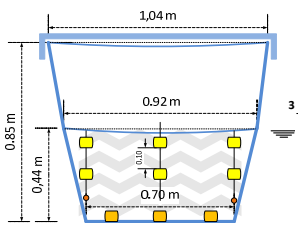	21 (20 correctly collected data)	2 min/data 588 data points per sensor	19.2 h From 17:43 pm to 12:40 am
October 2011 276 kg of depulped coffee cherries	 Inside a wharehouse	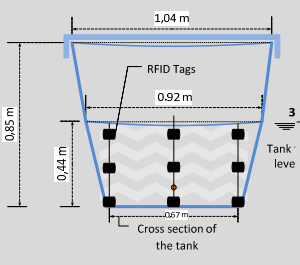	27 (23 correctly collected data)	2 min/data 504 data points per sensor	16.8 h From 17:00 pm to 9:50 am

The multidistributed sensor network consisted of TurboTag® RFID Tags temperature loggers; each Tag was protected by a resistant plastic material to guarantee the impermeability, as to avoid electrical shortcut derived from immersion in the fermenting mass. To remove the insulating effect of the air within the protective bag, it was drawn out through vacuum. The range and accuracy of temperature RFID tags is from -30ºC to +40ºC ± 0.5ºC. All communications with T-700 series tags are carried out

using an RFID reader DR-1 (RFID Interface 13.56 MHz). This is a small desktop USB device for use with a PC that runs with Session Manager Software. Due to an internal memory available of 702 data points, it used a high temporal resolution (Table 1). The sensors were equi-spatially distributed along 8 radii (Table 1), and three horizontal planes parallels to the floor (ground, medium and surface levels). On each plane 8 sensors were placed at 0.33m and one more at center (9 tags/plane), except for the ground plane in F_{OUT} where only were installed 3 tags at 0.15m of radius. Due to battery failure and/or configuration mistakes in F_{IN} 2 perimeter tags on medium plane (Figure 4) and 2 tags more at surface plane and in F_{OUT} 1 tag located on medium plane did not recorded correctly the data. An additional tag was placed out of the vat in both fermentations to register the ambient temperature.

Data analysis

In order to facilitate the handling of data from the 23 RFID Tags in F_{IN} and from the 20 RFID Tags in $F_{OUT,}$ a hierarchical clustering based on temporal series was performed to define groups of sensors. The matrix of Euclidean distances between each pair of individuals was calculated, grouping the closest individuals and hierarchically merging groups (or individuals) whose combination gave the smallest average linkage distance (that is, average distance between all pairs of objects in any two clusters). A MatLab® devoted code was developed to generate groups of sensors on the basis of the cluster tree features. To analyze recorded data two different and complementary procedures were implemented.

First, polar interpolation using dedicated Matlab code was developed as to make 2D spatial representations of the temperature profiles corresponding to the three horizontal planes defined in the tank. Prior knowledge on the location of each tag in the plane allowed defining the polar coordinates values: radius (0 cm or 33 cm) and angle (0 to 2π radians at 2π/8 radians steps), and generating an interpolation mesh grid (resolution of spatial mesh increase by one order of magnitude). The interpolation mesh grid is used under the Matlab function INTERP2 to compute the interpolated temperature values, at the points defined in the new mesh grid. In those polar coordinates where the RFID tags did not recorded temperature data, the average of temperatures between the previous and next polar coordinate was consigned previously to the interpolation operation. The function INTERP2 returns interpolated values of a function of two variables at specific query points using linear interpolation. The results always pass through the original sampling of the function. In the input of the function it have to be consigned the coordinates of the sample points, the values of the temperature in these points and the coordinates of the interpolation mesh grid. The Matlab function CONTOURF allows drawing 2-D surface plots with isolines representing equal temperatures and areas between isolines using constant colors. In our case 50 and 150 steps between the minimum and the maximum temperatures registered during the fermentation process were represented.

Secondly, the reconstruction of the phase space from the time series was carried out as is described in (Correa et al., 2014). Following Eckmann and Ruelle [see Sec. II-G in (Eckmann and Ruelle, 1985)], the best way to reconstruct the phase space from a time series is by using *time delays*. The technique is as follows. Let be the experimental time series $Y_1^{(k)} = y_1(t_k)$, with $k = 1, 2, \ldots, M$, corresponding to M periodic measures (i.e., measures with fixed time step $\tau = t_{k+1} - t_k$) of the physical magnitude y_1. Then, we can reconstruct the whole phase space including the remaining magnitudes $(y_1, y_2, \ldots, y_N)$, in the discrete form of the corresponding time series $(Y_1^{(k)}, Y_2^{(k)}, \ldots, Y_N^{(k)})$, by making $Y_i^{(k)} = Y_1^{(k+\Delta_i)}$ with $i = 1, 2, \ldots, N$ and $\Delta_1 = 0$, where each non negative integer Δ_i defines a time delay $t_{d_i} = t_{k+\Delta_i} - t_k = \Delta_i \cdot \tau$. In this work, two-dimensional ($N = 2$) phase space representations have been obtained by plotting the measured temperature $T(k)$ at each time $t(k)$ versus the temperature $T(k+\Delta)$ at time $t(k+\Delta)$, with optimum $\Delta = 10$ set up by heuristics. In this case, the data acquisition interval (i.e., the fixed time step of the time series) is $\tau = 2$ min., so that the corresponding

time delay is $t_d = \Delta \cdot \tau = 20$ min. The area of the trajectory loops corresponding to one sensor or group of sensors has been computed by using the Matlab function *convhulln*. The software STATISTICA 6.1 (StatSoft, Inc) and the statistical toolbox of Matlab® version 7.0 (R14) were used to compute basic statistics as the mean, standard deviation and standard error and to carry out the analysis of variance.

Results and Discussion

Temporal information

Table 2 presents the dynamic of temperatures inside the vats registered by RFID tags along the complete fermentation process. Taking into account all data, the average fermentation temperature for F_{OUT} (n=20 Tags) was 20.3ºC while for F_{IN} (n=23 Tags) was 21.2ºC, values similar to that reported by Avallone et al. (Avallone et al., 2001) for a 20 h fermentation under similar conditions. In both cases, the temperature inside the tanks was higher than outside during most of the fermentation step due to the activity of the mesophile microflora as referred in previous studies (Avallone et al., 2001). The lowest temperature registered was for F_{OUT} 18.3ºC and for F_{IN} 19.0ºC, while the maximum temperature was registered in the surface plane of the vats in both cases (23.2ºC for F_{OUT} and 23.6ºC for F_{IN}). As corresponds to a fermentation process that takes place spontaneously under ambient temperature conditions, lower external temperatures induce minor fermentation temperatures and a decrease in microorganism kinetics delaying the end of the fermentation, being the fermentation time 2.4 hours longer for $F_{OUT.}$

The average standard deviation was for F_{OUT} ±0.6ºC (SD, n=20 sensors) and for F_{IN} ±0.36ºC (SD, n=23 sensors), indicating that along this fermentation the temporal variability of the temperature or intrasensor variablity is lower than in F_{OUT}. On the other hand, the average spatial SD calculated for sensors at different locations for the same instant, was for F_{OUT} ±0.64ºC (n=588 time data) while F_{IN} doubled that value (±1.21ºC, n=504 time data), showing that the spatial temperature variability or variability intersensor was higher in this second fermentation.

In the clustering procedure five groups were identified in both fermentations (Table 3). In F_{IN} groups were labeled from A to E. Group A, consisting of 3 RFID Tags, corresponds to the hottest locations inside the tank (surface and medium plane at the center). Group B corresponding to 10 RFID Tags refers to peripheral location at surface and medium plane. Group C only includes one sensor near to the average fermentation temperature and located in the medium plane. Group D with 7 RFID Tags located at the floor of the tank. Finally group E with 2 sensors at the coldest location on floor plane.

In F_{OUT} groups were labeled from F to J. Group F, consisting of 2 RFID Tags, corresponds to the hottest locations inside the tank (surface and medium plane at the center). Group G corresponding to 4 RFID Tags refers to peripheral location at surface and medium plane. Group H with 5 RFID Tags, 3 located at the floor of the tank and 2 in peripheral location at medium plane. Group I with 4 RFID Tags at peripheral location at surface plane. Finally group J with 4 sensors at surface and medium plane which reached the coldest temperatures. The one-way analysis of variance (ANOVA) carried out (Figure 2) showed that the five groups selected in both fermentations were significantly different (F_{IN} with $F=72.16$ and F_{OUT} with $F=11.18$, $p<0.05$), identifying locations of different temperature behavior in the tank along the fermentation process.

Spatial information

A two-way ANOVA was carried out to analyze the effect of two factors: height and radial distance with no significative interaction in both fermentations. In F_{IN} the analysis showed that height had a relevant effect ($F=41.4$, $p<0.05$) on fermentation temperature with a decreasing vertical temperature gradient from the top of the vat to the floor (Figure 3), however this effect was not found in F_{OUT}. On the other hand, the radial distribution of sensors (center and peripheral) was significative and similar in

both fermentations, for F_{IN} F=17.9 ($p<0.05$) and F_{OUT} with F=16.9 ($p<0.05$), and indicated that the highest values of temperature were reached at the center of the vat (Figure 3).

Table 2. *(left) Dynamics of temperature inside the vat along the fermentation step, each colored line corresponds to one RFID Tag. (right) Red line represents the temperature registered outside the tank. Thin blue line shows the average instant temperature and thick blue lines the average instant standard deviation (n=20 sensors for F_{OUT} and n=23 sensors for F_{IN}) along the fermentation process.*

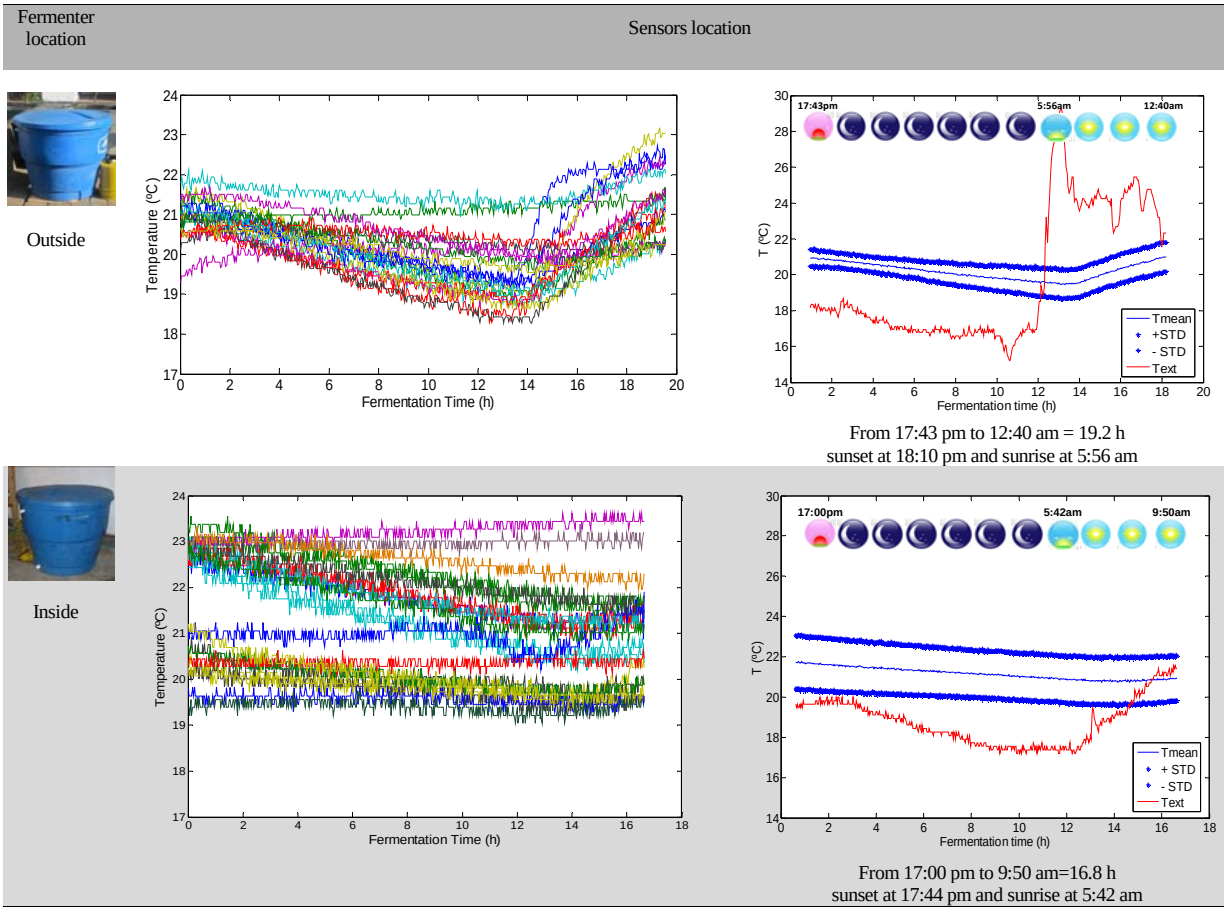

Table 3*. Shows the RFID Tags clustered by group, its placement in the tank at different heights or levels (M: medium, S: surface, F: Floor) and on the radius (C: center, P: perimeter). The correlation coefficient r of pearson for each Tag located inside the tank with respect to the Tag located outside is also shown (red color indicates a significant correlation).*

	F_{IN}																					
Group	**A**			**B**										**C**	**D**							**E**	
Tag ID	5	12	20	1	2	3	4	9	10	11	19	22	24	16	6	7	13	14	17	18	21	8	23
Level	M	S	S	S	S	S	M	S	M	S	M	M	M	M	F	F	F	F	F	F	F	F	F
Radius position	C	C	P	P	P	P	P	P	P	P	P	P	P	P	P	P	P	P	P	C	P	P	P
r	0.16	0.00	0.01	0.26	0.14	0.18	0.21	0.09	0.18	0.21	0.23	0.12	0.21	0.36	0.10	0.17	0.55	0.19	0.24	0.15	0.17	-0.04	0.26

	F_{OUT}																				
Group	**F**		**G**				**H**					**I**					**J**				
Tag ID	9	11	1	5	6	15	7	12	16	17	20	2	4	8	19	3	10	13	14	18	
Level	M	S	M	M	S	S	F	F	M	F	M	S	S	S	S	M	M	S	S	M	
Radius position	C	C	P	P	P	P	P	P	P	P	P	P	P	P	P	P	P	P	P	P	
r	0,65	0,07	0,53	0,39	0,24	0,41	-0,70	-0,18	-0,56	-0,49	-0,48	-0,27	-0,29	-0,09	-0,33	0,21	0,15	-0,20	0,07	-0,09	

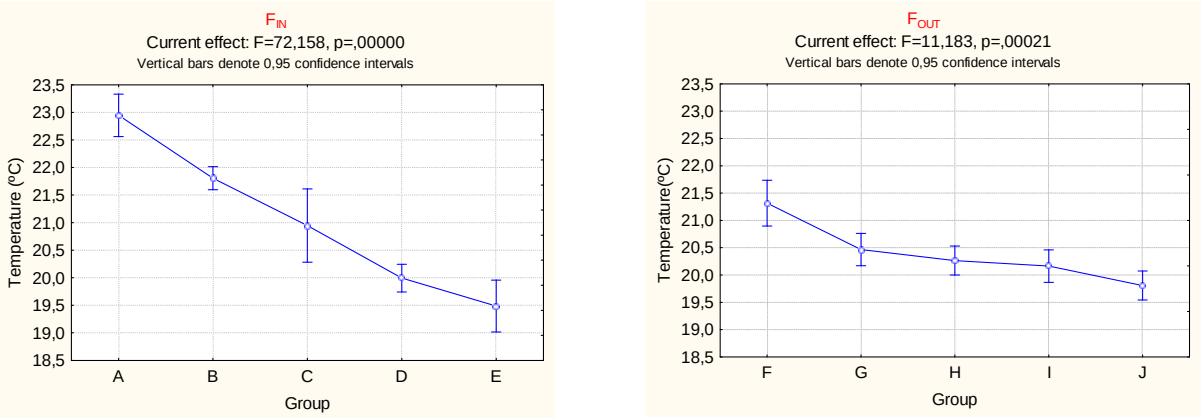

***Figure 2**. Least-squares mean graphs present the results of the one-way ANOVA and show the effect of factor "Group of sensors" on the variable "Temperature".*

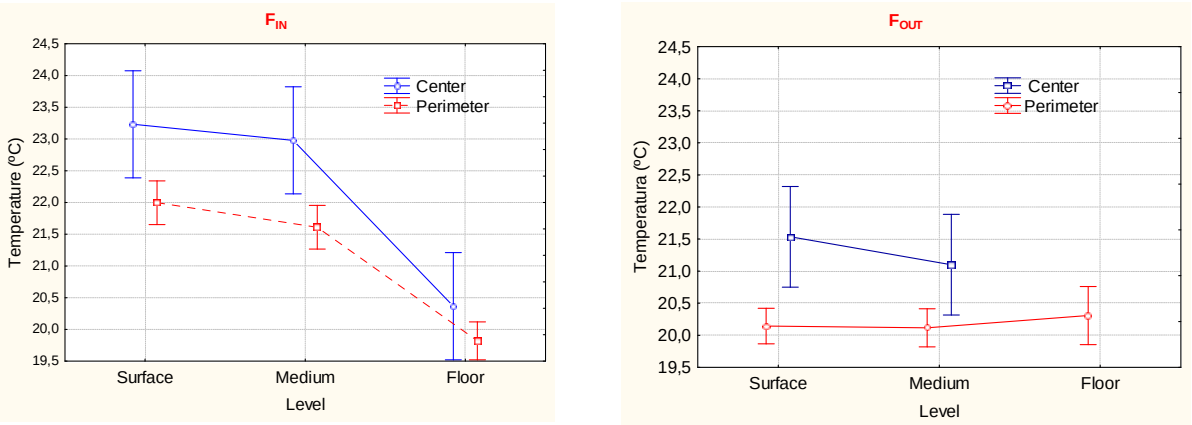

***Figure 3**. Least-squares mean graph presents the result of the two-way ANOVA and shows the effect of the factors "Level" or placement of sensors in the tank at different heights (surface, medium or floor) and placement of sensors at the radius (center or perimeter) on the variable "Temperature". Vertical bars denote 0.95 confidence intervals.*

The existence of those temperature gradients is corroborated by Figure 4 that shows the spatial distribution of temperatures in each plane of the tank at the beginning, the middle and the end of the fermentations process. At time t=0, the beans heated due to mechanical removal of pulp, were transferred to the fermentation vat. At this step temperature is high and homogeneous compared to other fermentation steps, which takes place over night. At this time only the bottom of the vat presents lower temperature than the other two planes due to the heat conduction through the concrete floor. Figure 4 shows that along the fermentation process surface and medium plane maintain a similar temperature profile. In F_{IN} the main vertical gradient of temperature occurs from the medium plane to the floor plane, between them the average temperature difference is 2ºC in 15 cm height, with a maximum instant variation of 3.8ºC for sensors with equal polar coordinates (temperature gradients of 0.25ºC/cm). Such variation is comparable to that found in other fermentation processes (red wine) where automated control is recommended based on vertical temperature gradients instead of time control. Ranasinghe et al. (Ranasinghe et al., 2013) limits to 5ºC the maximum vertical allowed variation. While in F_{OUT} due to sensors setup in the vat, it is not possible to calculate the vertical gradient between the medium and floor planes at locations with equal polar coordinates. This calculus made between the surface plane and medium plane reaches a maximum vertical gradient of 1.6ºC in 29 cm (0.055ºC/cm), much lower than those found for F_{IN}. Figure 4 also shows that for every plane and every fermentation time there is a radial gradient of temperatures as corresponds to a radial heat transfer from a pseudo-cylindrical vat to the surrounding air. The maximum instant radial gradient of temperatures has been quantified as 0.1ºC/cm from the center to the perimeter of the tank in both fermentations (3.3 ºC for F_{IN} and 3.2 ºC for F_{OUT}, in 33 cm of radius). Also in Figure 4, once the fermentation begins, at the middle and at the end of the process, images corresponding to surface plane

and medium plane are defined with a progressively higher number of contour lines than for the floor plane, indicating higher gradients for the former compared to the latter.

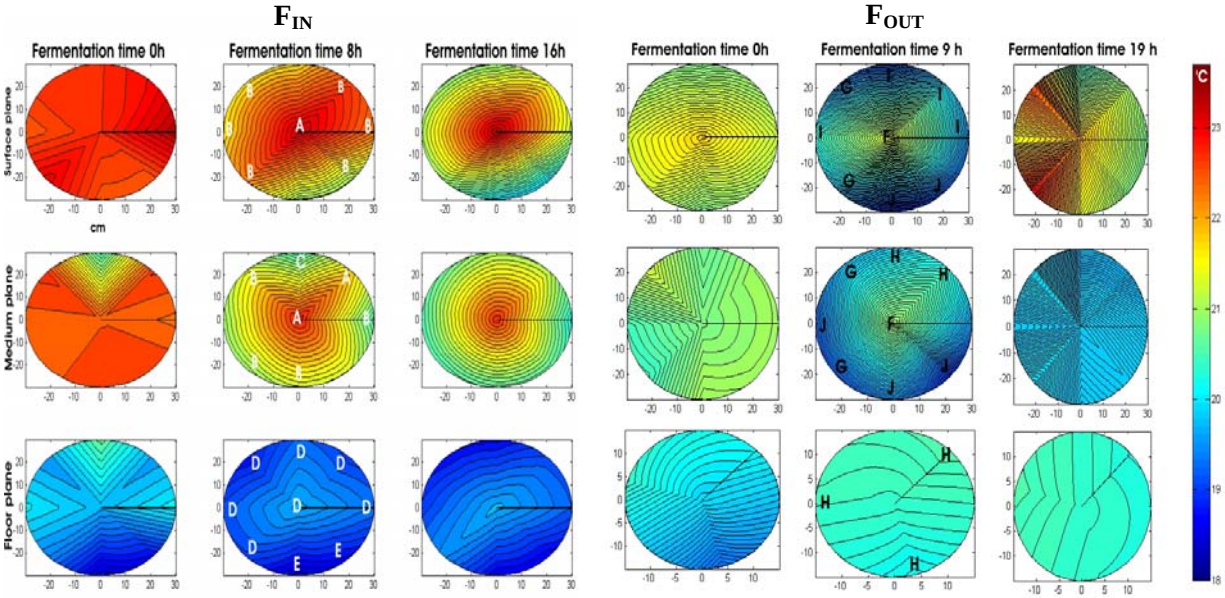

Figure 4. *2D surface plot of the temperatures interpolated along the radius of the tank (0-33 cm) for the three planes or height levels defined in the vat (surface, medium and floor). Three time instants have been selected, the beginning of the fermentation step (time 0 hours), the middle and the end of the fermentation process. The location of the sensors on each plane according to the group to which they belong is also shown.*

On the other hand, Figure 5(up) shows the phase graph of temperature series along the complete fermentation (Δ=10, $t_d = 10(\text{step})\cdot 2(\text{min/step}) = 20\text{min}$) for the five clusters of sensors identified in both fermentations. Sensors belonging to the same group appear in the same color and in the same region of the phase graph .The areas of the polygons that include all the data points of each individual sensor on phase graph quantify the variability of the temperature for each location. Groups A and F with an average temperature of 22.9ºC and 21.3ºC respectively, refer to the hottest points of the tank located mainly in the center of the vat. Those sensors also characterize one of the most stable temperature areas of the tank as indicated by the small average area on the phase space (0.39 $^oC^2$ in F_{IN} and 0.51 $^oC^2$ in F_{OUT}, Δ=10; Figure 6 down).

With respect to the floor of the vat, groups D plus E and H are clustering sensors located on the floor plane, showing a small average area (0.57 $^oC^2$ in F_{IN} and 0.56 $^oC^2$ in F_{OUT}, Δ=10; Figure 6 down). This identified the floor plane with one of the more stable temperature locations inside the vat. Groups D and E showed an average temperature of 19.7 ºC and are located on the base of their phase graph (Figure 6 up), thus they provide the coldest points when the vat is placed inside the warehouse. This is due to the heat conduction to the concrete floor of the warehouse which is colder than the quasi-static air surrounding the vat. On the other hand, group H is located in a medium position in its phase graph with an average temperature of 20.3ºC and is identifying a location where the temperature is stable and high throughout the fermentation process F_{OUT}. This is due to the heat conduction to the concrete floor of the outdoor, soil stays warmer than the air streams surrounding the vat during night. Groups B, G, I and J that include peripheral RFID Tags located at the surface and medium plane, can be identified as the zones subjected to the highest temperature gradients as shown by their largest average area on the phase space, 1.1 $^oC^2$ for group B in F_{IN} and 2.3 $^oC^2$ for groups G, I and J in F_{OUT} (Δ=10; Figure 6 down). This is especially remarkable in the case of the group G in F_{OUT}, which presents an area of 3 $^oC^2$. The direct exposition of this area to the air streams surrounding the vat makes it the most affected for the external ambient conditions, as it is corroborated by the highest average coefficient of correlation r=0.4, found for the sensors of this group with the external tag.

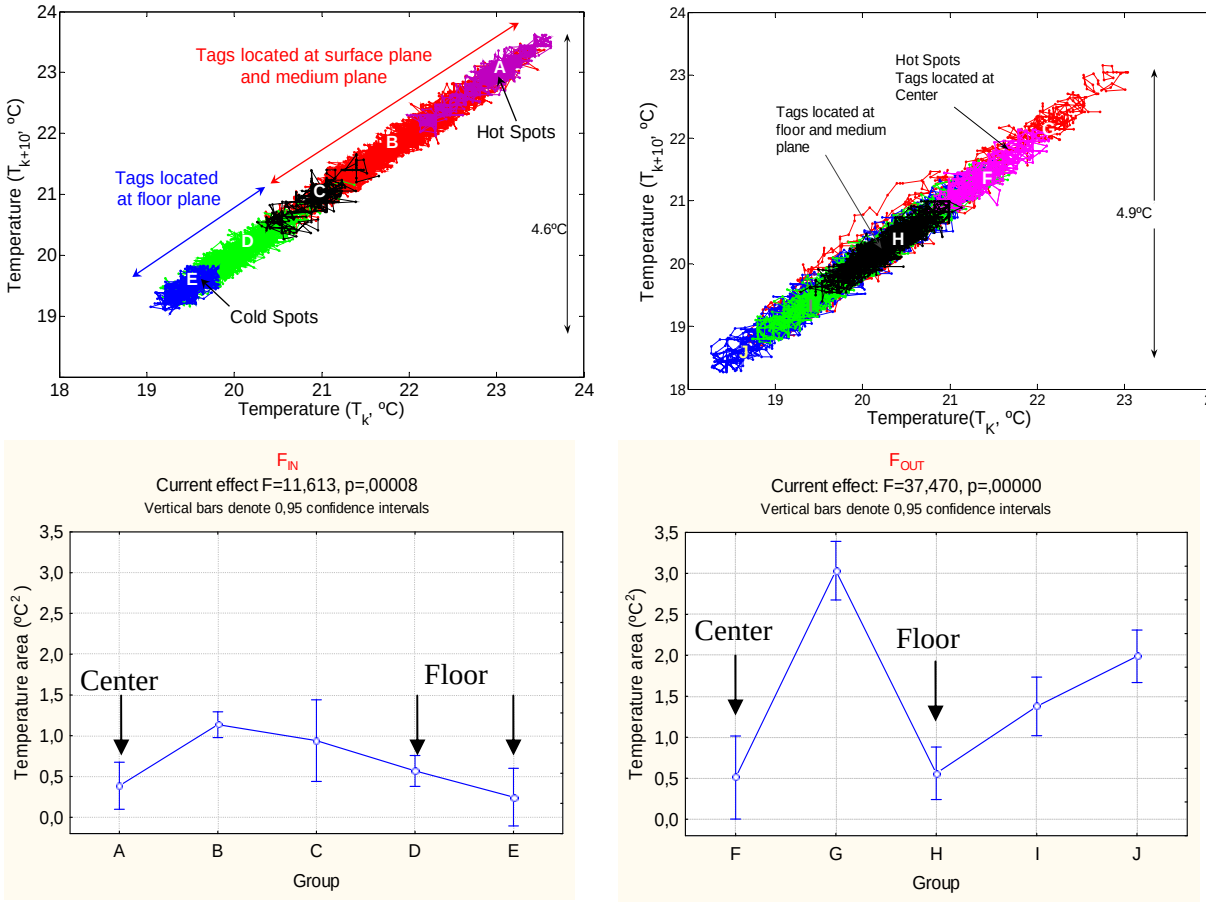

***Figure 5**. (Up) Phase graph for temperature with Δ=10 ($t_d = 10(\text{step})\cdot 2(\text{min/step}) = 20\text{min}$) for RFID Tag sensors in F_{IN} (left): group A (magenta), group B (red), group C (black), group D (green) and group E (dark blue); and in F_{OUT} (right) group F (magenta), group G (red), group H (black), group I (green) and group J (dark blue). (Down) Least-squares mean graphs present the result of the one-way ANOVA showing the effect of the factor "Group of sensors" on the variable "Temperature area" corresponding to the areas computed on the phase graph shown in the upper part of this figure for each sensor.*

Conclusions

This work shows spatial interpolation and phase space graphs as novel methodologies that demonstrate that significative temperature gradients occur within coffee fermenting tanks. The use of these two complementary methodologies allows identifying a variety of consistent behaviors during fermentation that can be quantitatively characterized. The maximum range of temperature variation has been bounded by RFID Tags higher than 4.5ºC in both fermentations. Spatial interpolation shows that there is a consistent radial gradient of temperature that has been quantified as 0.1ºC/cm from the center to the perimeter of the tank. Phase graphs of temperatures allow the recognition of hot and cold spots. The area of the attractors computed within the temperature phase graphs is used as an indicator of the temperature variability. The average area for peripheral tags (1.1 $ºC^2$ for F_{IN} and 2.3 $ºC^2$ in F_{OUT}) located at surface and medium plane, identifying the zone of the vat subjected to the highest variations of temperature. On the other hand, the floor plane and the center of the vat, with areas that can reach values between 4 and 6 times minors, are identifying the locations in the vat with higher temperature stability. The temperature gradients found are the results of two combined effect: 1) the heat dissipation from a tank without isolation by convection towards the outside environment mainly in radial direction, and by conduction to the concrete floor, and 2) the different kinetics of the exothermic reactions depending on the distribution of temperatures and nutrients in the fermenting mass. The two fermentations supervised are characterized to heterogeneous temperature fermentation along the process and a strong influence of the external ambient conditions. This could result in heterogeneity of

fermented grain aromatic compounds that will influence the sensory characteristics of the coffee cup. The lack of control favors the development of sensory defects in the final product, since they may lead to local over-fermentations in hot spots together with incomplete fermentations at the coldest locations.

Acknowledgments

This study was funded by the Spanish Government through SMART-QC project (GL2008-05267-C03-03), UPM projects COFFEE-ONLINE (AL15-PID-12) and CAFECOL (AL11-PID-30) and the International Net of CYTED FRUTURA (109RT0383). We wish to thank too for their support to the companies SUPRACAFÉ_España and SUPRACAFÉ_Colombia and their staffs, the Technical University of Madrid and the International Campus of Excellence CEI Moncloa/UPM-UCM.

References

Avallone, S., Guyot, B., Brillouet, J. M., Olguin, E., and Guiraud, J. P. (2001). Microbiological and biochemical study of coffee fermentation. *Current Microbiology* **42**, 252-256.

Barreiro, P., Correa, E. C., Arranz, F. J., Diezma, B., Ruiz-García, L., Villarroel, M., Robla, J. I., and García-Hierro, F. J. (2010). Smart Sensing Applications in Agriculture and Food. *In* "Smart Sensors: Technology, Developments and Applications" (I. N. Y. Nova Science Publishers, ed.).

Bede-Wegner, H., Bendig, I., W., H., and R., W. (1997). Volatile compounds associated with the over-fermented flavour defect. *In* "17th International Scientific Colloqium on Coffee", pp. 176-182. Association Scientifique Internationale du Café (ASIC), Nairobi.

Correa, E. C., Jimenez-Ariza, T., Diaz-Barcos, V., Barreiro, P., Diezma, B., Oteros, R., Echeverri, C., Arranz, F. J., and Ruiz-Altisent, M. (2014). Advanced Characterisation of a Coffee Fermenting Tank by Multi-distributed Wireless Sensors: Spatial Interpolation and Phase Space Graphs. *Food and Bioprocess Technology* **7**, 3166-3174.

Di Gennaro, S. F., Matese, A., Primicerio, J., Genesio, L., Sabatini, F., Di Blasi, S., and Vaccari, F. P. (2013). Wireless real-time monitoring of malolactic fermentation in wine barrels: the Wireless Sensor Bung system. *Australian Journal of Grape and Wine Research* **19**, 20-24.

Eckmann, J. P., and Ruelle, D. (1985). Ergodic-theory of chaos and strange attractors. *Reviews of Modern Physics* **57**, 617-656.

Esteban-Diez, I., Gonzalez-Saiz, J. M., and Pizarro, C. (2004). Prediction of sensory properties of espresso from roasted coffee samples by near-infrared spectroscopy. *Analytica Chimica Acta* **525**, 171-182.

Garcia, R., Arriola, D., Dearriola, M. C., Deporres, E., and Rolz, C. (1991). Characterization of coffee pectins. *Food Science and Technology-Lebensmittel-Wissenschaft & Technologie* **24**, 125-129.

Illy, A., and Viani, R. (2005). "Espresso Coffe: The Chemistry of Quality," Academic Press Limited, U.K.

Jackels, S. C., and Jackels, C. F. (2005). Characterization of the coffee mucilage fermentation process using chemical indicators: A field study in Nicaragua. *Journal of Food Science* **70**, C321-C325.

Lopez, C. L., Bautista, E., Moreno, E., and Dentan, E. (1989). Factors related to the formation of ‘overfermented coffee beans‘ during the wet processing method and storage of coffee. *In* "13th" (A. S. I. D. C. (ASIC), ed.), pp. 373-384, Paipa, Colombia.

Masoud, W., and Jespersen, L. (2006). Pectin degrading enzymes in yeasts involved in fermentation of Coffea arabica in East Africa. *International Journal of Food Microbiology* **110**, 291-296.

Murthy, P. S., and Naidu, M. M. (2011). Improvement of Robusta Coffee Fermentation with Microbial Enzymes. *European Journal of Applied Sciences* **3**, 130-139.

Mussatto, S. I., Machado, E. M. S., Martins, S., and Teixeira, J. A. (2011). Production, Composition, and Application of Coffee and Its Industrial Residues. *Food and Bioprocess Technology* **4**, 661-672.

Peñuela-Martínez, A. E., Oliveros- Tascón, C. E., and Sanz-Uribe, J. R. (2010). Remoción del mucílago de café a través de fermentación natural. *Cenicafé* **61**, 159-173.

Ranasinghe, D. C., Falkner, N. J. G., Chao, P., and Hao, W. (2013). Wireless Sensing Platform for Remote Monitoring and Control of Wine Fermentation. *In* "2013 Ieee Eighth International Conference on Intelligent Sensors, Sensor Networks and Information Processing" (M. Palaniswami, C. Leckie, S. Kanhere and J. Gubbi, eds.), pp. 503-508.

Sainz, B., Antolin, J., Lopez-Coronado, M., and de Castro, C. (2013). A Novel Low-Cost Sensor Prototype for Monitoring Temperature during Wine Fermentation in Tanks. *Sensors* **13**, 2848-2861.

Woelore, W. M. (1993). Optimum fermentation protocols for Arabica coffee under Ethiopian conditions. *In* "15th International Scientific Colloqium on Coffee" (A. s. i. d. c. (ASIC), ed.), pp. 727-733, Montpellier.